PROCEEDINGS

HANOI UNIVERSITY OF SCIENCE AND TECHNOLOGY
INTERNATIONAL TRAINING INSTITUTE FOR MATERIALS SCIENCE

# PROCEEDINGS ICAMN 2019

## THE 4TH INTERNATIONAL CONFERENCE ON ADVANCED MATERIALS AND NANOTECHNOLOGY

OCTOBER 13-16, 2019


HANOI, VIETNAM

ISBN: 978-604-950-978-0

## CONTENTS

# Microstructure, magnetic and electrical properties of (La, Ni) co-doped $BiFeO_3$ materials

**Dao Viet Thang[1,2*], Nguyen Manh Hung[1,2], Le Thi Mai Oanh[2], Du Thi Xuan Thao[1], Bui Dinh Tu[3], Bui Thi Thu[2], and Nguyen Van Minh[2]**

[1]Department of Physics, Hanoi University of Mining and Geology, North Tuliem District, Hanoi, Vietnam
[2]Center for Nano Science and Technology, Hanoi National University of Education, 136 Xuan Thuy Road, Cau Giay District, Hanoi, Vietnam
[3]Faculty of Engineering Physics and Nanotechnology, VNU-University of Engineering and Technology, 144 Xuan Thuy Road, Cau Giay District, Hanoi, Vietnam
*Corresponding author: daovietthang@humg.edu.vn

***Abstract:*** **-Multiferroics $BiFeO_3$ (BFO), Ni doped $BiFeO_3$ (BFNO), and (La, Ni) co-doped $BiFeO_3$ (BLFNO) materials were synthesized by sol-gel method. Effects of Ni-doping and (La, Ni) co-doping on structural, magnetic and electrical properties of BFO materials were investigated by different techniques as X-ray diffraction (XRD), energy dispersion X-ray (EDX), Raman scattering, magnetization hysteresis loops (*M-H*), and complex impedance spectra measurement. Analysis results of XRD measurement shows that all samples crystallize in the rhombohedral structure with $R_{3C}$ space group. The BFO sample has crystal lattice parameters $a$ = 5.580 Å, $c$ = 13.865 Å and average crystal size $L_{XRD}$ = 58 nm. The BFNO sample has $a$ = 5.582 Å, $c$ = 13.868 Å and $L_{XRD}$ = 55 nm. However, BLFNO samples have crystal lattice parameters $a$, $c$ and $L_{XRD}$ decrease when concentration of La increases. Results of Raman scattering spectra shows that the peaks position characterize of Bi-O covalent bonds shifted toward higher frequency when concentration of La increases, which confirms that La substitutes into Bi-site. Magnetization hysteresis loops measurement indicates all samples present weak ferromagnetic behavior. BFO sample presents weak ferromagnetic behavior with saturation magnetization $M$s = 0.037 emu/g and remnant magnetization $M$r = 0.004 emu/g. The $M$s and $M$r values of co-doping samples enhance compare to that of BFO. Origin ferromagnetism of materials will be discussed in this report.**

***Keywords:*** X-ray, Raman, (La, Ni) co-doped, ferromagnetic, impedance.

## I. INTRODUCTION

Multiferroics materials coexist ferromagnetic (antiferromagnetic), ferroelectric, ferroelastic orders, and magneto-electric (ME) effect in the same structure phase, which have been reported by previous studies [1-4]. Therefore, these materials can be used application in electronic device as store information, memory, sensor, ultrasonic broadcast. However, the competition between ferromagnetic and ferroelectric orders lead to the multiferroics materials are very rare in nature.

$BiFeO_3$ (BFO) is one of multiferroics materials nature coexists both anti-ferromagnetic order ($T_N$ ~ 643 K) and ferroelectric order ($T_C$ ~ 1100 K) [3]. However, BFO has small saturation magnetization and polarization electric at room temperature, which limits the applicability of this materials. This problem may be solved by modification magnetic and electric properties of BFO. Previous studies showed that magnetization of BFO was improved by substitution of rare earth ions ($Gd^{3+}$, $Ho^{3+}$, $Sm^{3+}$, $Nd^{3+}$, etc.) into Bi-sites [5-7] or transition metal ions ($Ni^{2+}$, $Co^{2+}$, $Mn^{2+}$, etc.) into Fe-sites [8-10]. Recently, some studied showed that both ferromagnetic and ferroelectric properties enhanced when rare earth and transition metal ions co-doped into BFO host materials [11-13].

In this work, we to choose La and Ni co-doped into BFO. Because La-doped $BiFeO_3$ presented improved dielectric properties, Ni substitution for Fe-site can affect magnetic properties to greater extent and that may be large ME effect at room temperature [14, 15]. Our results will indicate the change structural, magnetic and electric properties of BFO when La and Ni substitute into Bi-sites and Fe-sites, respectively.

## II. EXPERIMENTAL

The pure $BiFeO_3$, Ni doped $BiFeO_3$, and (La, Ni) co-doped $BiFeO_3$ materials were synthesized by sol-gel method. The chemicals used $Bi(NO_3)_3.5H_2O$, $Fe(NO_3)_3.9H_2O$, $La(NO_3)_3.6H_2O$, $Ni(NO_3)_2.6H_2O$, ethylene glycol solution $C_2H_6O_2$, and citric acid. Firstly, the $Bi(NO_3)_3.5H_2O$, $Fe(NO_3)_3.9H_2O$, $La(NO_3)_3.6H_2O$, and $Ni(NO_3)_2.6H_2O$ were soluble in 35 ml citric acid solution. Then, the solution mixed by magnetic stirrer at temperature range 50 ÷ 60 °C in 45 minutes obtained to sol. The next, temperature of the sol was increased up to 100 °C to evaporation water, which obtained to wet gel after 3 hours. The

gel was dried at temperature 130 °C in 4 hours. Finally, dry gel was annealed at temperature 800 °C in 7 hours obtained powders materials.

The microstructures, magnetic and electrical properties of all samples were investigated by X-ray diffraction (XRD, Equinox 500), energy dispersion X-ray (EDX, Quanta 450), Raman scattering (LabRAM HR Evolution, λ = 532 nm), magnetization hysteresis loops (M-H, Lake Shore Cryotronics Westerville, 7404), and complex impedance spectra (LeCroy equipment and LabView 8.0 software).

## III. RESULTS AND DISCUSSION

The chemical composition of pure BFO and $Bi_{1-x}La_xFe_{0.97}Ni_{0.03}O_3$ ($x$ = 0.00, 0.05, 0.10 and 0.15) powders investigated by EDX measurement, as are shown in Fig 1. As see in Fig. 1, EDX spectra of BFO sample appears characteristic peaks for Bi, Fe and O elements. The EDX spectra of Ni-doped $BiFeO_3$ ($x$ = 0.00) appears characteristic peaks for Bi, Fe, O, and Ni elements while that of (La, Ni) co-doped samples appear characteristic peaks for Bi, Fe, O, Ni and La elements. Intensity of characteristic peaks of La increases as concentration of La increases. This is initial information, which is necessary to study physical properties of all the samples.

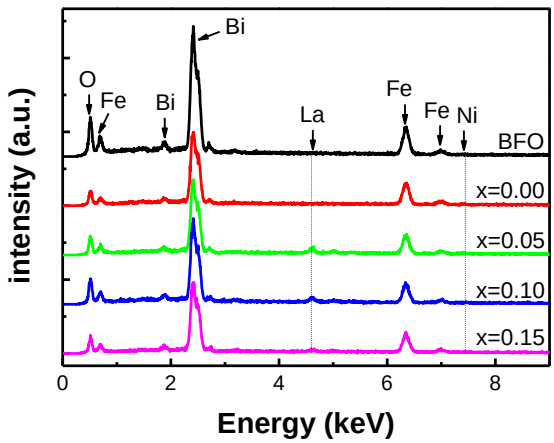


**Figure 1.** EDX spectra of BFO and $Bi_{1-x}La_xFe_{0.97}Ni_{0.03}O_3$ ($x$ = 0.00, 0.005, 0.10 and 0.15) powders.

The phase formation and crystal structure of BFO and (La, Ni) co-doped BFO materials are investigated by XRD measurement. Fig. 2a shows X-ray diffraction diagram of BFO and (La, Ni) co-doped BFO powders. The XRD pattern of the all samples exhibit rhombohedral structure of $BiFeO_3$ crystal structure (JPCDS No. 71-2494). The main peaks can be indexed to the (012), (104), (110), (006), (202), (024), (116), (122), (018), and (300) reflections, as are shown in Fig. 2a.

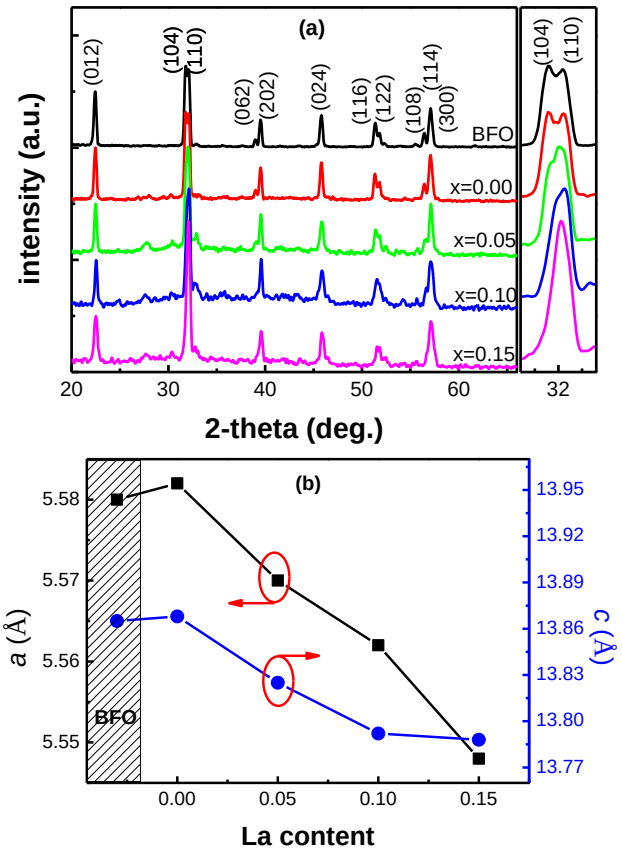


**Figure 2.** XRD patterns of BFO and $Bi_{1-x}La_xFe_{0.97}Ni_{0.03}O_3$ ($x$ = 0.00, 0.05, 0.10, and 0.15) powders.

The XRD patterns shows that $La^{3+}$ and $Ni^{2+}$ ions are well dissolved into the BFO crystal lattice. However, the effect of (La, Ni) co-doping into crystal structure of BFO may be observed by comparing the location of (012), (104), and (110) diffraction peaks, as are inserted in Fig 2a. The diffraction peaks of sample with $x$ = 0.00 shifts toward lower $2\theta$ compare to that of BFO.

From data of XRD measurement, crystal lattice parameters and average crystalline size ($L_{XRD}$) have been determined by using UnitCell software and Sherrer's formula, as are shown in Table 1. As see in Table 1, the BFO sample has crystal lattice parameters $a$ = 5.580 Å, $c$ = 13.865 Å and average crystalline size $L_{XRD}$ = 58 nm, the Ni-doped sample has crystal lattice $a$ = 5.582 Å, $c$ = 13.868 Å and average crystalline $L_{XRD}$ = 55 nm. While the crystal lattice parameters and average crystalline size of (La, Ni) co-doped samples decrease when concentration of La increases. The observation can be easily understood due to the larger ionic radius of $Ni^{2+}$ (0.69 Å) compare to that of $Fe^{3+}$ (0.65 Å). For (La, Ni) co-doped

samples, the diffraction peaks position shifts toward higher $2\theta$ compare to that of sample $x$ = 0.00, which could be explained the smaller ionic radius of $La^{3+}$ (1.16 Å) compare to that of $Bi^{3+}$ (1.17 Å) [14].

**Table 1.** Crystal lattice parameters and average crystalline size of BFO and $Bi_{1-x}La_xFe_{0.97}Ni_{0.03}O_3$ samples.

| Samples | $a$ (Å) | $c$ (Å) | $L_{XRD}$ (nm) |
|---|---|---|---|
| BFO | 5.580 | 13.865 | 58 |
| $x$ = 0.00 | 5.582 | 13.868 | 55 |
| $x$ = 0.05 | 5.570 | 13.825 | 50 |
| $x$ = 0.10 | 5.562 | 13.792 | 47 |
| $x$ = 0.15 | 5.548 | 13.788 | 35 |

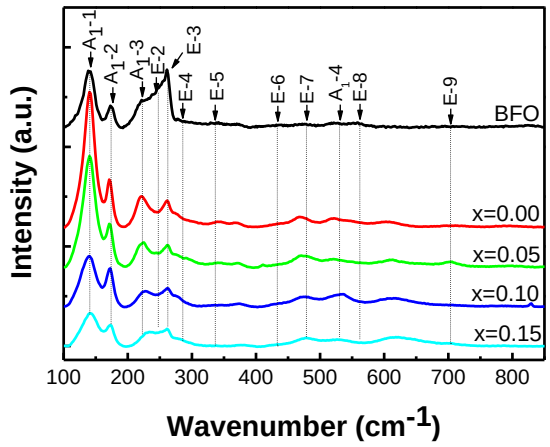


**Figure 3.** Raman scattering spectra of BFO and $Bi_{1-x}La_xFe_{0.97}Ni_{0.03}O_3$ ($x$ = 0.00, 0.05, 0.10, and 0.15) materials.

Raman scattering spectra of BFO and $Bi_{1-x}La_xFe_{0.97}Ni_{0.03}O_3$ samples in the range of 100 ÷ 800 $cm^{-1}$ at room temperature are shown in Fig. 3. The spectrum of pure BFO has twelfth Raman modes at 139, 173, 225, 252, 262, 285, 336, 433, 474, 521, 555, and 706 $cm^{-1}$. They are signed as in Fig. 3. The modes frequencies are in good agreement with other reports. Previous studies showed that the modes at low frequency characterize to Bi-O bonds, while the modes at high frequency characterize to Fe-O bonds [16]. For Ni-doped sample ($x$ = 0.00), the position of *E*-2, *E*-3, *E*-4, and *E*-5 modes shift toward higher frequency, the position of *E*-8, *E*-9 modes shift toward lower frequency compare to that of pure BFO. Analysis Raman scattering of (La, Ni) co-doped samples indicate that the position of $A_1$-1, $A_1$-2, $A_1$-3, $A_1$-4, *E*-3, *E*-6, *E*-7, *E-8*, and *E*-9 modes shift toward higher frequency compare to that of Ni-doped sample. Previous studies showed that the $A_1$ and *E* modes at lower frequency characterize to Bi-O covalent bonds, other *E* modes characterize to Fe-O covalent bonds [14, 17]. The change position of Raman modes confirms $La^{3+}$ and $Ni^{2+}$ ions substitute into Bi-sites and Fe-sites, respectively. This result is consistent with XRD result, which shows $La^{3+}$ and $Ni^{2+}$ co-doped into BFO lead to decrease crystal lattice parameters.

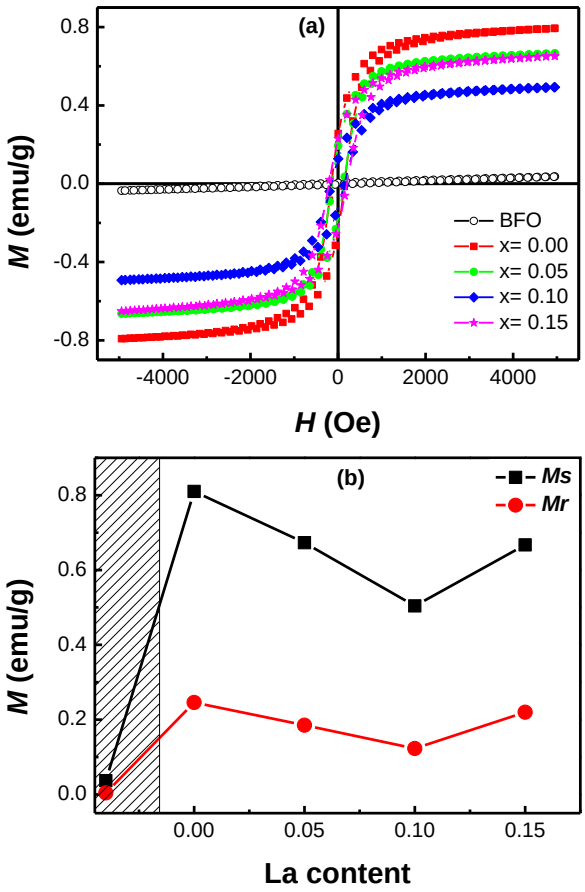


**Figure 4.** Magnetization hysteresis loop of BFO and $Bi_{1-x}La_xFe_{0.97}Ni_{0.03}O_3$ materials.

Fig. 4a shows magnetization hysteresis loops of $BiFeO_3$ and $Bi_{1-x}La_xFe_{0.97}Ni_{0.03}O_3$ samples. As see in Fig. 4a, all samples present weak ferromagnetic behavior. Saturation magnetization (*Ms*) and remnant magnetization (*Mr*) of BFO are 0.037 emu/g and 0.004 emu/g, respectively. The *Ms* and *Mr* of Ni doped sample ($x$ = 0.00) increase up to 0.810 emu/g and 0.246 emu/g, respectively. It is understood due to Ni substitutes into Fe-sites to appear double exchange interaction $Fe^{3+}$-$O^{2-}$-$Ni^{2+}$ and oxygen vacancies leading to increase of the magnetization [18, 19]. Analysis magnetization hysteresis loops of (La, Ni) co-doped samples indicates the *Ms* and *Mr* of these samples decrease compare to that of $x$ = 0.00 sample when concentration of La increases. However, the *Ms* and *Mr* of (La, Ni) co-doped samples is higher

than that of BFO sample. As see in Fig. 4b, both *Ms* and *Mr* decrease when concentration of $La^{3+}$ increases from $x$ = 0.00 to $x$ = 0.10. When concentration of $La^{3+}$ increases up to $x$ = 0.15 both *Ms* and *Mr* slight increases. It can be explained La substituted into Bi-sites lead to decrease double exchange interaction $Fe^{3+}$ - $O^{2-}$ - $Ni^{2+}$ and oxygen vacancy. This can be reason make to decrease magnetization.

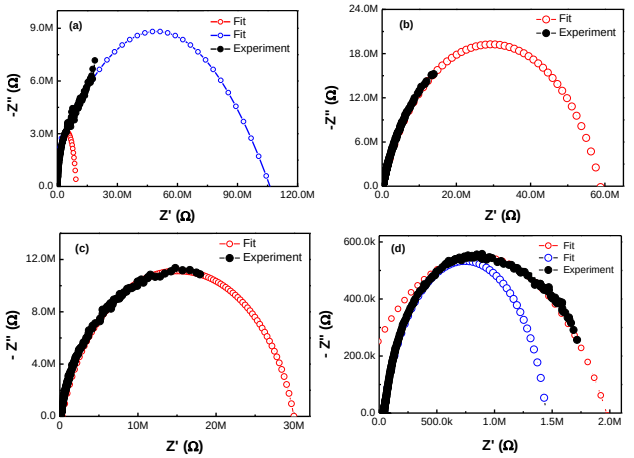


**Figure 5.** Impedance spectra of $BiFeO_3$ and $Bi_{1-x}La_xFe_{0.97}Ni_{0.03}O_3$ materials: (a) $BiFeO_3$; (b) $x$ = 0.00; (c) $x$ = 0.05; (d) $x$ = 0.15.

Complex impedance spectra of $BiFeO_3$ and $Bi_{1-x}La_xFe_{0.97}Ni_{0.03}O_3$ materials are shown in Fig. 5. Analysis complex impedance spectra of materials may be known grain internal, grain boundaries, and electrode interface contributions. Previous studies showed that the complex impedance spectra of materials exhibit successive semicircles in the complex plane. A low frequency semicircle is due to ion and electrode, an intermediate frequency semicircle gives information on the grain boundary and/or impurity-phase impedance. While a high frequency semicircle originates from the grain internal. Some previous studies showed all these contributions may be not all detected. Fig. 5a presents impedance spectra of BFO, which include a semicircle at high frequency tend toward zero and a semicircle at intermediate frequency not tend toward zero in the complex plane. These semicircles are determined contribution of grain internal and grain boundary, respectively. The impedance spectra of co-doped samples with $x$ = 0.00, 0.05, and 0.10 is similar, which include a semicircle at high frequency tend toward zero in the complex due to contribution of grain internal, as are shown in Fig. 5b, c. When concentration of $La^{3+}$ increases up to $x$ = 0.15, the change crystal lattice lead to change impedance of this sample. As see in Fig. 5d, the impedance of $x$ = 0.15 sample includes two semicircles contribution by grain internal and grain boundary.

## IV. CONCLUSION

In summary, we have synthesized successful $BiFeO_3$ and (La, Ni) co-doped $BiFeO_3$ materials by sol-gel method. We have studied effect of La and Ni co-doping on crystal structure, magnetic and electrical properties. Results of XRD and Raman scattering measurement confirmed $La^{3+}$ and $Ni^{2+}$ ions substituted into Bi-sites and Fe-sites, respectively. It makes to crystal lattice parameters and crystalline size decrease when concentration of $La^{3+}$ increases. Analysis result of magnetization hysteresis loops shows that all samples present weak ferromagnetic behavior. Pure $BiFeO_3$ sample presents ferromagnetic behavior with saturation magnetization and remnant magnetization are 0.037 emu/g and 0.004 emu/g, respectively. Magnetic properties of (La, Ni) co-doped samples improved compare to that of pure $BiFeO_3$.

## ACKNOWLEDGMENT

The work has been supported by the Ministry of Education and Training of Vietnam (Code: B2018-MDA-02-CtrVL). The authors also thank the support of Hanoi University of Mining and Geology (Code: T19-04).

## REFERENCES

[1] W. Eerenstein, N.D. Mathur, and J.F. Scott, Multiferroic and magnetoelectric materials, *Nature*, 442 (2006) 759-765.

[2] C. Ederer and N.A. Spaldin, Weak ferromagnetism and magnetoelectric coupling in bismuth ferrite, *Phys. Rev. B*, 71 (2005) 060401(R).

[3] P. Ravindran, R. Vidya, A. Kjekshus, H. Fjellvåg, and O. Eriksson, Theoretical investigation of magnetoelectric behavior in $BiFeO_3$, *Phys. Rev. B*, 74 (2006) 224412.

[4] S.W. Cheong and M. Mostovoy, Multiferroics: a magnetic twist for ferroelectricity, *nat. mater.*, 6 (2007) 13-20.

[5] M. Kumarn, P.C. Sati, S. Chhoker, and V. Sajal, Electron spin resonance studies and improved magnetic properties of Gd substituted $BiFeO_3$ ceramics, *Ceram. Int.*, 41 (2015) 777–786.

[6] X. Zhang, Y. Sui, X. Wang, Y. Wang, and Z. Wang, Effect of Eu substitution on the crystal structure and multiferroic properties of $BiFeO_3$, *J. Alloy. Compd.*, 507 (2010) 157-161.

[7] S.K. Pradhan, J. Das, P.P. Rout, V.R. Mohanta, S.K. Das, S. Samantray, D.R. Sahu, J.L. Huang, S. Verma,

and B.K. Roul, Effect of holmium substitution for the improvement of multiferroic properties of $BiFeO_3$, *J. Phys. Chem. Solids*, 71 (2010) 1557-1564.

[8] H. Naganuma, J. Miura, and S. Okamura, Ferroelectric, electrical and magnetic properties of Cr, Mn, Co, Ni, Cu added polycrystalline $BiFeO_3$ films, *Appl. Phys. Lett.*, 93 (2008) 052901.

[9] Y.R. Dai, Q. Xun, X. Zheng, S. Yuan, Y. Zhai, and M. Xu, Magnetic properties of Ni-substituted $BiFeO_3$, *Physica B*, 407 (2012) 560–563.

[10] G. Dong, G. Tan, Y. Luo, W. Liu, H. Ren, and A. Xia, Optimization of the multiferroic $BiFeO_3$ thin films by divalent ion (Mn, Ni) co-doping at B-sites, *Mater. Lett.*, 118 (2014) 31-33.

[11] D. Viet Thang, L. Thi Mai Oanh, N. Cao Khang, N. Manh Hung, D. Danh Bich, D. Thi Xuan Thao, and N. Van Minh, Structural, magnetic and electric properties of Nd and Ni co-doped $BiFeO_3$ materials, *AIMS Mater. Sci.*, 4 (2017) 982-990.

[12] D.V. Thang, N.M. Hung, D.T.X. Thao, L.T.M. Oanh, D.D. Bich, N.C. Khang, V.Q. Nguyen, and N.V. Minh, Structural, Electrical, and Magnetic Properties of $Bi_{0.90}Nd_{0.10}Fe_{0.98}TM_{0.02}O_3$ ( TM = Mn, Co, Ni, and Cu) Materials, *IEEE Mag. Lett.*, 10 (2019) 2501505.

[13] X. Yan, G. Tann, W. Liu, H. Ren, and A. Xia, Structural, electric and magnetic properties of Dy and Mn co-doped $BiFeO_3$ thin film, *Ceram. Int.*, 41 (2015) 3202–3207.

[14] A. Kumar, P. Sharma, W. Yang, J. Shen, D. Varshney, and Q. Li, Effect of La and Ni substitution on structure, dielectric and ferroelectric properties of $BiFeO_3$ ceramics, *Ceram. Int.*, (2016).

[15] S.S. Rajput, R. Katoch, K.K. Sahoo, G.N. Sharma, S.K. Singh, R. Gupta, and A. Garg, Enhanced electrical insulation and ferroelectricity in La and Ni co-doped $BiFeO_3$ thin film, *J. Alloy.Compd.*, 621 (2015) 339–344.

[16] M. Cazayous, D. Malka, D. Lebeugle, and D. Colson, Electric field effect on $BiFeO_3$ single crystal investigated by Raman spectroscopy, *Appl. Phys. Lett.*, 91 (2007) 071910.

[17] G.L. Yuan, S.W. Or, and H.L. Chan, Raman scattering spectra and ferroelectric properties of $Bi_{1-x}Nd_xFeO_3$ (x = 0-0.2) multiferroic ceramics, *J. Appl. Phys.*, 101 (2007) 064101.

[18] Y. Gu, J. Zhao, W. Zhang, S. Liu, S. Ge, W. Chen, and Y. Zhang, Improved ferromagnetism and ferroelectricity of La and Co co-doped $BiFeO_3$ ceramics with Fe vacancies, *Ceram. Int.*, 42 (2016) 8863-8868.

[19] J.S. Park, Y.J. Yoo, J.S. Hwang, J.H. Kang, B.W. Lee, and Y.P. Lee, Enhanced ferromagnetic properties in Ho and Ni co-doped $BiFeO_3$ ceramics, *J. Appl. Phys.*, 115 (2014) 013904.